



Catalytic Activity of Modified Electrodes in Fuel Cells. I. The Electrochemical Behavior of Rhenium under Natural Corrosion Conditions



Mahmoud G. A. Saleh¹, S. Abd El Wanees^{*2,3}, Syed Khalid Mustafa⁴

¹Department of Chemistry, Faculty of Science, Northern Border University, Arar, Saudi Arabia

²University Collage of Umilij, Tabuk University, Tabuk, Saudi Arabia

³Chemistry Departement, Faculty of Science, Zagazig University, Zagazig, Egypt

⁴Department of Chemistry, Faculty of Science, University of Tabuk, Tabuk, Saudi Arabia

THE corrosion behavior of Re microelectrode in several aqueous solutions has been inferred from open circuit capacitance, C , and potential, E , measurements in the absence and presence of O_2 , at 25°C. Inspection of the steady-state potential, E_{st} reveals that the metal surface is covered by an oxide film whose composition is likely to be ReO_2 . In all examined solutions except H_3PO_4 , and CH_3COOH , the pre-immersion surface oxide film dissolves, whereas in these latter two solutions it grows. The presence of the dissolved oxygen acts bi-functionally on the rhenium electrode. Its effect is more pronounced in the slightly corrosive solutions such as Na_2SO_4 . The rate of oxide film growth has been measured in acetic acid solutions and found to increase directly with the acid concentration. The relative thickness of the formed oxide film at the steady-state condition (after about 90 minutes of immersion), viz. C^{-1} at ac frequency, $f = 20$ k Hz, increases with c .

A comparison of the oxide formation rates coefficients derived from capacitance measurements with those derived from potential measurements reveals that the oxide structure change with the solution composition; probably the degree of hydration of the oxide decreases with an increase of acid concentration, c .

Complex plane analysis of the impedance gives the dielectric loss angle of the oxide. It was found to be in the range 40 - 58° for c in the range 1.0 - 50 mM. The formed modified rhenium oxide electrode indicates a good catalytic activity towards the oxidation of methanol in acidic solutions.

Keywords: Rhenium, Electrochemical behavior, Catalytic activity, Modified electrode, Oxide film.

Introduction

Interest in rhenium and its oxides is increasing due to the possibility of alloying with either of the valve metals to activate their oxides or with the noble ones to stabilize their oxides [1]. Thus, an alloy containing rhenium hopeful will achieve the required properties (durability and reactivity) in the technologically important processes such as catalysis, electrochromism, corrosion, and energy conversion photocells [2]. Rhenium-

based materials [3-5] and Rhenium oxides [6, 7] are of interest in industrial and technological applications. Rhenium oxides have been mostly used in heterogeneous catalysis and fuel cells. Recently there has been an increased interest in applying these oxides to electro chromic devices [8], liquid crystal cells [7], fuel cells [9-11] and photoelectron chemical cells [12-14]. This is because their cost is lower than that of other materials, such as Pt, Pd or Rh.

*Corresponding author e-mail: s_wanees@yahoo.com

Received 24/12/2019; Accepted 8/6/2020

DOI: 10.21608/ejchem.2020.21382.2278

©2020 National Information and Documentation Center (NIDOC)

A complete review of the previous works on rhenium is given earlier [15]. The electrochemistry of pure rhenium needs more understanding, as it seems to be complicated. This complexity is probably due to:

- i- Its electronic configuration. It is intermediate between those of the valve metals and the noble ones.
- ii- It has several stable oxidation states, a matter that gives rise to several products under open-circuit conditions or upon anodization.
- iii- It has an intermediate metal-oxygen bond energy [16].

Early investigations by Hefny *et al.* [17] on the behavior of rhenium in aqueous solution reveal that:

- i- The pre-immersion oxide film dissolves directly in the concentrated sulfuric acid solutions but after a hydration step in the dilute ones [17-19].
- ii- The porosity of the anodic oxide film changes with the anodization potential.
- iii- Repetitive cyclic scanning increases the charge capacity of the cyclic voltammogram due to the formation of a hydrated oxide film.

In HCl of concentration less than 7.0 M, the pre-immersion oxide film dissolves while the more concentrated solutions indicates an oxide film development [17]. In weak acid media, the presence of chloride ions assists the dissolution of the pre immersion oxide, while in the weak alkaline ones; it assists the growth of the aqueous oxide film. A mechanism for the dissolution process in HCl has been deduced.

The aim of the present study is the elucidation of the behavior of rhenium in different solutions using capacitance measurements. Capacitance is a more reliable and sensitive propose for the reactivity of the surface of the corrosion-resistant metals such as rhenium than potential. The catalytic activity of the formed rhenium oxide electrode towards the electro-oxidation of methanol is examined.

Experimental

Reagent grade chemicals and triple distilled water were used in solutions preparations. Solutions were de aerated by bubbling pure nitrogen or oxygen for half an hour before each experiment. A saturated calomel reference

electrode and a counter platinum sheet electrode for impedance measurements were used. The potential of the rhenium electrode was measured vs a calomel electrode (SCE) by means of a valve voltmeter (Electronic Instruments Ltd, England). The electrode capacitance C was measured by means of a high precision standardized bridge of the Wien type. The bridge and electrolytic cell were essentially the same as described before [19, 20]. The input a.c. voltage to the bridge was always 10 mV. The bridge was standardized using standard capacitance and resistance and the divergence was $< 1\%$ being within the tolerance of the standards used.

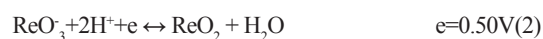
A high internal impedance voltmeter was used for potential measurements. Potentials were measured while the leads to the Ac bridge were disconnected. The temperature of the cell was $25 \pm 1^\circ\text{C}$. The radius of the rhenium wire is 0.5 mm and its purity is 99.99 %. It was supplied from Johnson Matthey Inc. The wire was fixed in a capillary tube of appropriate radius by an Araldite resin so only the cross sectional area exposes the test solution. For each experiment, the electrode surface was mechanically polished with sand papers of increasing fineness until it become mirror bright. Then the electrode was washed by distilled water.

Measurements involve the determination of the electrode potential, E_h , capacitance, C , and series resistance, R , as a function of the immersion time, t . R and C were measured at the normal working frequency, viz 1 k Hz. Upon reaching, the steady state that took in most cases less than 90 minutes from the moment of immersion, the effect of frequency, f , on the components of the electrode impedance viz R and C was followed in the range 0.3 - 20 k Hz. Electrochemical polarization was made using a Wenking Potentiostan Type POS 73. The data of current density-potential curves were recorded on an X - Y recorder, Type Advance HR 2000.

Results and Discussion

Composition of the surface layer

The steady-state open circuit potentials of rhenium electrode in the different solutions lie in the potential region 0.25 - 0.369 vs. SCE (Table 1 and Fig. 1). This potential region is close to that in which the following two equilibria occur [15].



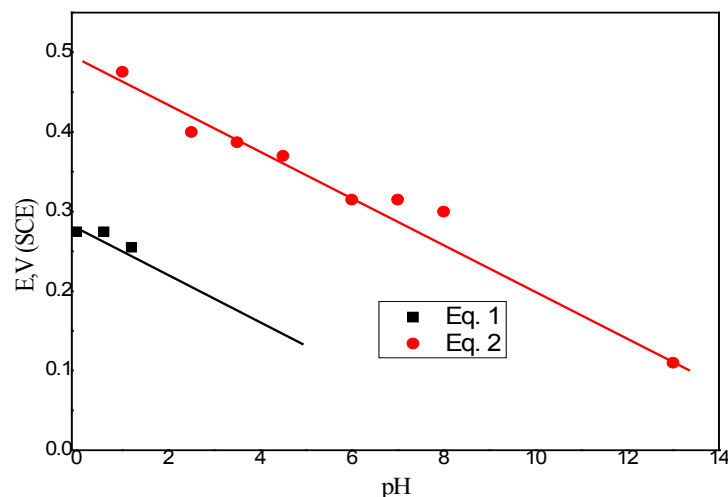


Fig. 1. Variation of the steady-state open circuit potentials of rhenium with pH of the solution. Eq. 1, $\text{ReO}_2 + 4\text{H}^+ + 4\text{e}^- \leftrightarrow \text{Re} + 2\text{H}_2\text{O}$ and eq. 2, $\text{ReO}_3 + 2\text{H}^+ + \text{e}^- \leftrightarrow \text{ReO}_2 + \text{H}_2\text{O}$.

TABLE 1. Variation of steady-state potentials, E_{st} (units in mV vs SCE) in 1.0 M solutions

1 M solution	E_{st} , V vs SCE	
	O_2	N_2
NaClO_4	0.254	0.260
NaNO_3	0.299	0.302
Na_2SO_4	0.312	0.317
NaCl	0.311	0.317
H_2SO_4	0.269	0.265
HNO_3	0.268	0.254
HClO_3	0.369	0.250
HCl	0.265	0.252
H_3PO_4	0.316	0.236
HCOOH	0.246	0.250
NaOH	0.131	0.135

Thus under the prevailing experimental condition, the metal is covered by an oxide layer which present in a state of equilibrium in the aqueous solutions [20].

Role of the medium

Fig. 2 shows the change of the open circuit capacitance, C , of the rhenium electrode with the immersion time, t , in the different solutions under N_2 de-aeration condition. A similar behavior has been observed in O_2 saturated solutions. In most solutions, C increases with t , this is possibly due to the dissolution of the pre-immersion oxide film on the rhenium surface. In few cases (CH_3COOH and H_3PO_4) C decreases with t , this indicates the further growth of the pre-immersion oxide film. For quantification of these trends a corrosion

coefficient, r , has been introduced, viz.

$$r = \frac{C_i^{-1} - C_f^{-1}}{C_f^{-1}} \quad (3)$$

where C_i^{-1} and C_f^{-1} are the inverse of the initial and the final capacitances, respectively, i.e., at $t = 1$ and $t = 90$ minutes, respectively. The last figure is the time limit of the experiment. When r is positive, it means that the oxide film dissolves and when it is negative, it means that it grows further during this period. At a given measuring ac frequency, f , C can be put as a function of each of the oxide thickness, X , roughness of the surface, σ , and reactivity of the surface towards the occurrence of charge transfer reaction, ξ , thus [21]:

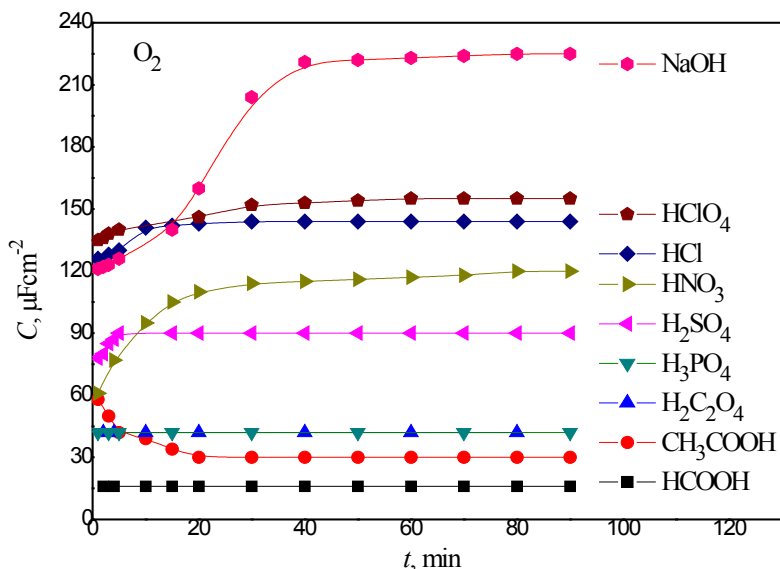


Fig. 2A. Variation of electrode capacitance, C , with immersion time, t , in various solutions saturated with O_2 .

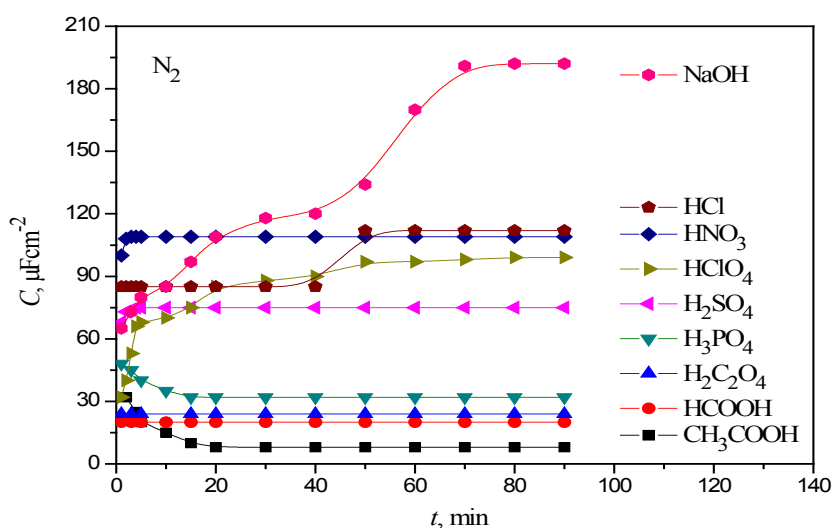


Fig. 2B. Variation of electrode capacitance, C , with immersion time, t , in various solutions saturated with nitrogen N_2 .

$$C = \frac{\epsilon}{4\pi X} + A\sigma + B\xi \quad (4)$$

where A and B are the proportionality constants

characteristic of the solution composition and ϵ is the dielectric constant of the oxide. In a solution of fixed composition, C changes with t due to the change of X . For the corrosion resistant metals such as rhenium [22], σ and ξ are hardly changed with time under open circuit conditions.

The corrosion coefficients of rhenium in the different solutions (under O_2 saturation, r_O or N_2

de-aeration, r_N) are given in Table 2, that reveal that:

- i- The rate of corrosion of rhenium in the studied solutions is maximum in NaOH and minimum in Na_2SO_4 .
- ii- The presence of oxygen enhances the dissolution process in the weakly corrosive solution, e.g., Na_2SO_4 .
- iii- The pre-immersion oxide film grows further in H_3PO_4 and largely in CH_3COOH .

TABLE 2. Variation of the corrosion coefficient r_o and r_N of Re in 1.0 M solutions at 25°C.

1 M solution	$r = (C_i^{-1} - C_r^{-1}) / C_r^{-1}$	
	r_o	r_N
NaOH	0.87	1.94
HClO ₄	0.15	1.5
HCl	0.14	0.34
HNO ₃	0.96	0.15
H ₂ SO ₄	0.16	0.17
H ₃ PO ₄	0.00	-0.24
CH ₃ COOH	-0.50	-0.73
HCOOH	0.00	0.00
NaCl	0.22	0.00
Na ₂ SO ₄	-0.03	0.25
NaNO ₃	-0.03	-0.50
NaClO ₄	0.00	0.33
H ₂ C ₂ O ₄	0.03	0.06

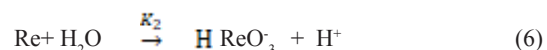
Acetic acid is a suitable medium for growth of the oxide film because it has the following features:-

- i- Weak electrolyte as compared to each of the strong electrolyte, NaOH, and HClO₄. In these two solutions, dissolution of the oxide film is relatively high [22].
- ii- Non-complexing acid as compared to the chloride-containing medium, in which dissolution is enhanced [18].
- iii- Non-oxidizing medium, hence oxidative dissolution of the oxide is forbidden, which seems to occur in HNO₃.

Growth of the oxide in acetic acid

Kinetics of the oxide, film formation on rhenium has been studied in solutions of acetic acid at pH 1.8, in presence of 0.05 M H₂SO₄. The results are shown in Fig. 3. In this figure C^{-1} , which is proportional with the oxide thickness [21] increases linearly with the logarithm of the immersion time, $\log t$. The slope of a given line, K_c is the oxide formation rate coefficient in the given medium [23]. K_c increases linearly with the acetic acid concentration, c , as shown in Fig 4. On the other hand, the pH of the medium within the range 0-3 does not influence on the oxide formations process, Figs 5 and 6.

The role of acetic acid in the oxide formation process can be elucidated as follows. Rhenium oxide grows as a net reaction for the following reactions:



When acetic acid is adsorbed on the electrode surface, it inhibits reaction (6) more than reaction (5) because O₂ adsorbs more strongly than water [24]. Assuming that hydration of the oxide (reaction 6) is the rate-determining step for the oxide dissolution whereas adsorption of oxygen (reaction 5) is the rate-determining step for the oxide formation process. Thus, the rate of oxide formation V is given by

$$V = K_1(Re)(O_2) - K_2(ReO_2)(H_2O) \tag{7}$$

where,

(Re) is the surface concentration of the active sites readily for oxide formation.

(O₂) is the degree of surface coverage by oxygen.

(ReO₂) is the surface concentration of the active sites readily for dissolution of the oxide.

(H₂O) is the degree of surface coverage by water.

Assuming that in the presence of acetic acid, the summation of the degrees of surface coverage is constant, K , thus:

$$(O_2) + (H_2O) + (CH_3COOH) = K \tag{8}$$

where (CH₃COOH) is the degree of surface coverage by acetic acid. From (7) and (8).

$$V = k_1(Re)(O_2) - k_2(ReO_2) [K - (CH_3COOH) - (O_2)] \tag{9}$$

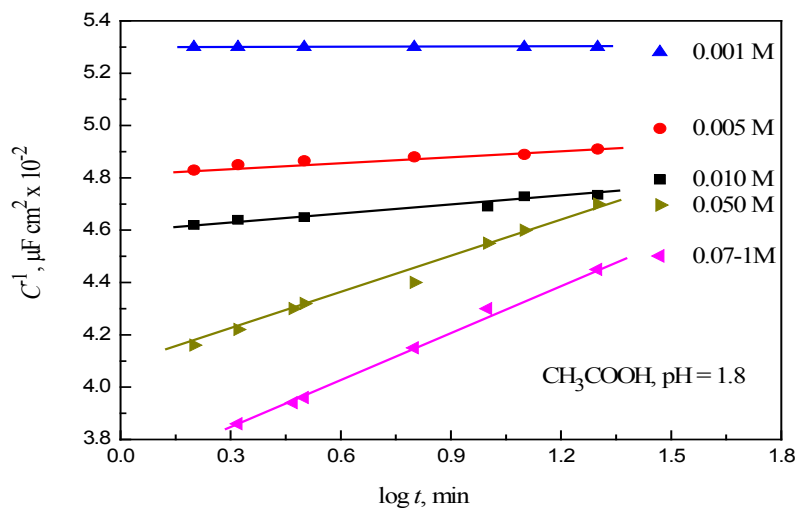


Fig. 3. Reciprocal capacitance, C^{-1} , against logarithm of the immersion time, t , for the rhenium electrode in solutions of different concentration of acetic acid (pH = 1.8)

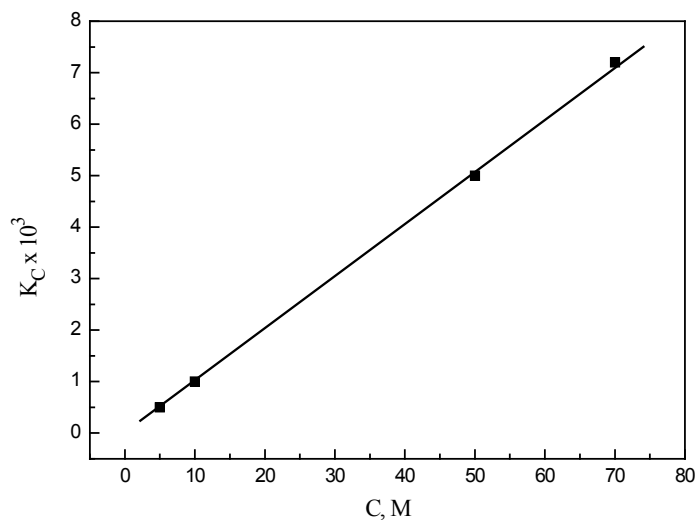


Fig. 4. Dependence of the rate of oxide formation k_c on acetic acid concentration, c .

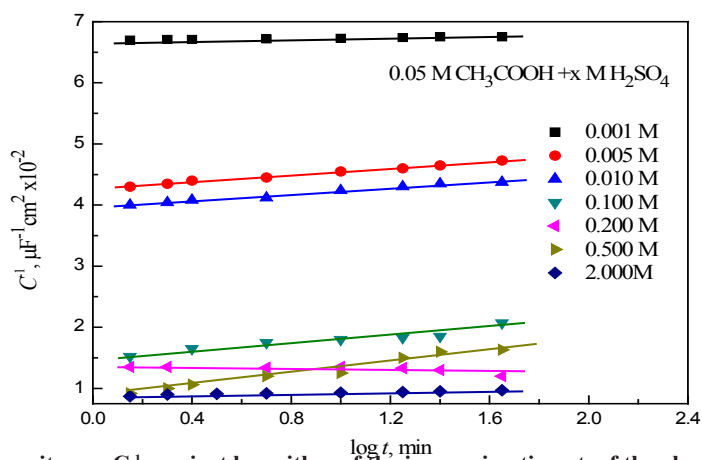


Fig. 5. Reciprocal capacitance, C^{-1} , against logarithm of the immersion time, t , of the rhenium electrode in 0.05 M $\text{CH}_3\text{COOH} + x \text{ M H}_2\text{SO}_4$.

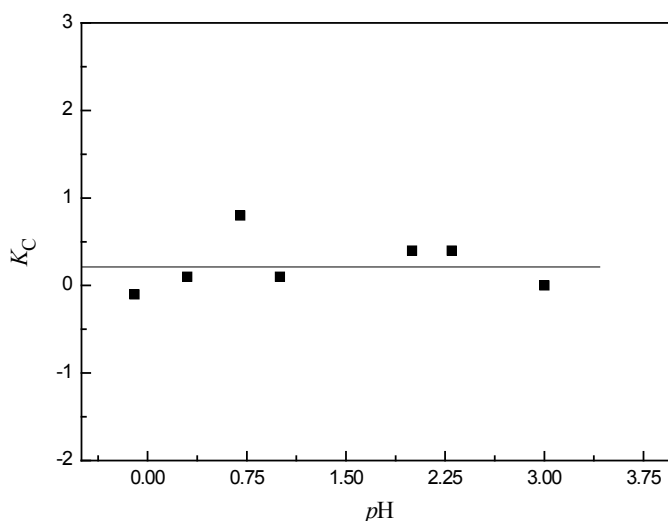


Fig. 6. Dependence of rate of oxide formation k_c on pH of the medium.

$$\frac{\partial V}{\partial(\text{CH}_3\text{COOH})} = K_c(\text{ReO}_2) \quad (10)$$

The last equation fits our experimental results, i.e., the rate of oxide formation, k_c increases linearly with acetic acid concentration as shown in Fig 4.

Assuming that the (CH_3COOH) is proportional to the concentration of acetic acid in the solution [25].

The results of open circuit potential (OCP) confirm those of capacitance measurements. Fig. 7 shows the increase of the rate of oxide formation as inferred from OCP, k_E . k_E is defined in the same way as k_c which are, respectively,

$$\frac{\partial E}{\partial \log t} \text{ and } \frac{\partial c^{-1}}{\partial \log t}. \text{ The increase of each of } k_E \text{ and } k_c \text{ with acetic acid concentration, } c \text{ is shown in Fig 8. This figure reveals that capacitance is a}$$

better prop than potential since $\frac{\partial k_c}{\partial c} > \frac{\partial k_E}{\partial c}$. This is possibly due to the open structure nature of the oxide. High metal-oxygen bond energy oxides only have compact structure [26].

Steady-state thickness

Another criterion for the oxide growth process in acetic acid is the steady state thickness of the oxide, X_{ss} . One can measure X_{ss} from equation (4) when C is measured at a suitably high frequency, e.g. > 10 kHz. Under this condition, the pseudo-capacitances due to the charge transfer reactions has been eliminated [21]. Hence, equation (4)

becomes $C \approx \frac{\epsilon}{4\pi X}$ since ϵ is unknown. One can give the relative thicknesses of the oxide in the different solutions, viz, C_{ss}^{-1} at $f = 15$ k Hz, Table (3). This table reveals that higher the concentration of the acetic acid, the thicker is the oxide film, C_{ss}^{-1} . This result accords with that derived from the evolution study, Figs 3-5.

Characteristics of the oxide

The previous sections show that rhenium oxide can grow in acetic acid solutions at what rate and the relative steady-state thicknesses. Beside this information, it is beneficial to get another type of information that is the quality of the oxide, e.g., its dielectric or insulating properties.

One of the techniques that can be employed for this purpose is the study of the impedance of the oxide, e.g., the Cole-Cole plots [27]. In one of its version (Nyquist), $(2\pi fC)^{-1}$ is plotted vs R , where R is the measured resistance associated with each C . At higher frequency, i.e., for f within the range 0.5 - 15 k Hz, the relation between $(2\pi fC)^{-1}$ and R can be approximated to a straight line whose slope gives the tangent of the angle of the dielectric loss of the oxide, $\tan \delta$, Fig 9 shows this plot. Table 4 includes the slope of the line as well as δ , as a function of c .

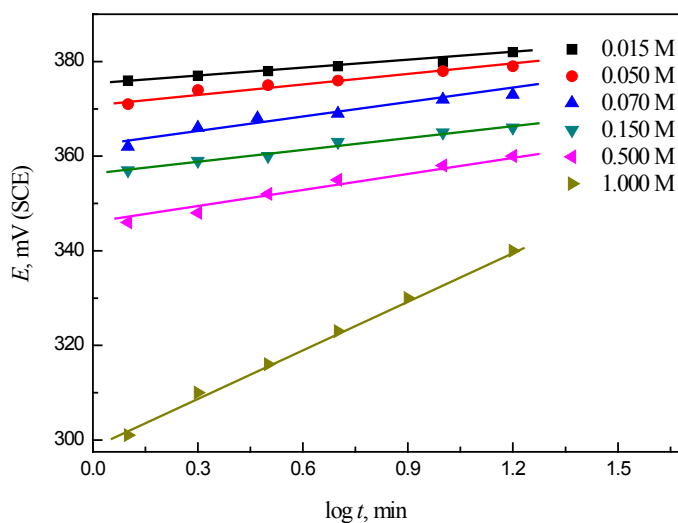
An inspection of the data in Table 4 indicates that the oxide grown in the concentrated solutions is more compact or less reactive than that grown in the dilute solutions. Alternatively, the oxide grown in the dilute solutions has more open

TABLE 3. The increase in the steady state capacitance, C , μFcm^{-2} with acetic acid concentration, c , at $f = 20$ kHz.

Concentration, c	C , μFcm^{-2}	$1/C$, $\mu\text{F}^{-1}\text{cm}^2$
0.001 M	0.032	31
0.010 M	0.032	31
0.050 M	0.024	42
0.070 M	0.0047	212

TABLE 4. The increase of the slope of the Nyquist curve, S and the dielectric loss angle, δ , with acetic acid concentration, c .

Concentration, c , M	S	δ
0.001 M	0.83	40
0.010 M	1.00	45
0.050 M	1.60	58

Fig. 7. Variation of open circuit potential, E , with logarithm of the immersion time, t , of Re electrode in different concentration of acetic acid.

structure, possibly due to its inclusion of higher amounts of H_2O .

Catalytic activity

The activity of the formed Re oxide electrode towards the electro-oxidation of methanol is investigated by potentiodynamic technique. Fig 10 represent the E - I curves for the modified Re electrode (after immersion at sufficient time in *Egypt. J. Chem.* **63**, No. 10 (2020)

0.05 M acetic acid) in 0.1 M CH_3OH in 0.5 M H_2SO_4 . It is clear that the current start to increase largely after 0.45 V as due to the reactivity of the formed rhenium oxide as a catalyst towards the oxidation of methanol according to the reaction [28].



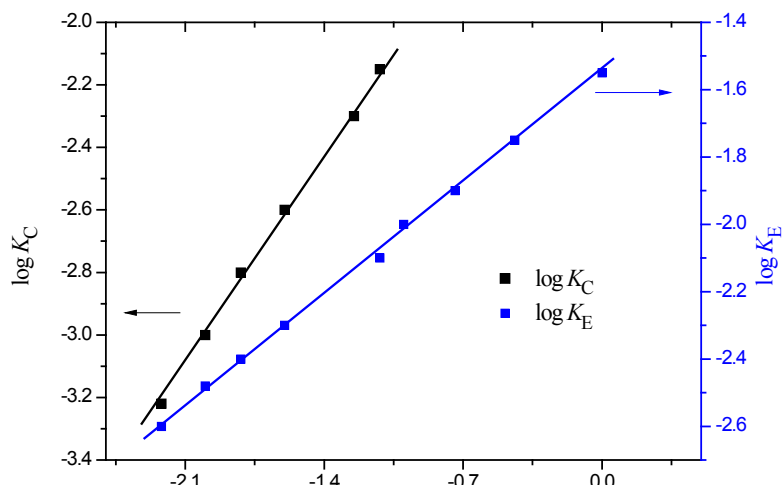


Fig. 8. Dependence of K_C and K_E on the acetic acid concentration, c .

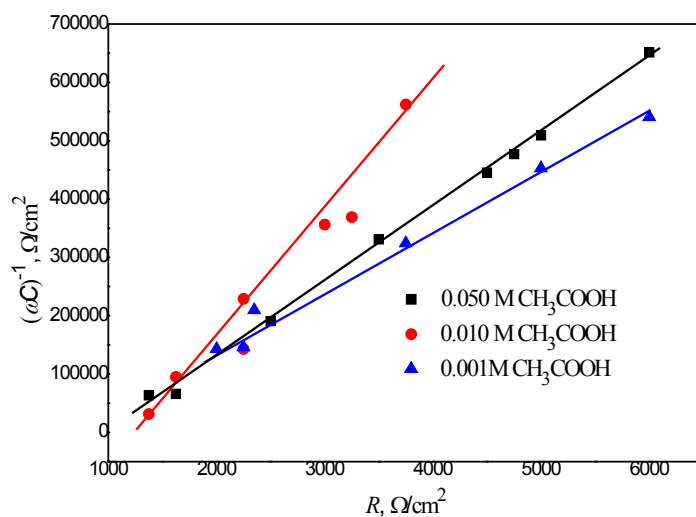


Fig. 9. Complex plane impedance plot of Re electrode (Nyquist curve) in different concentrations of CH_3COOH solutions.

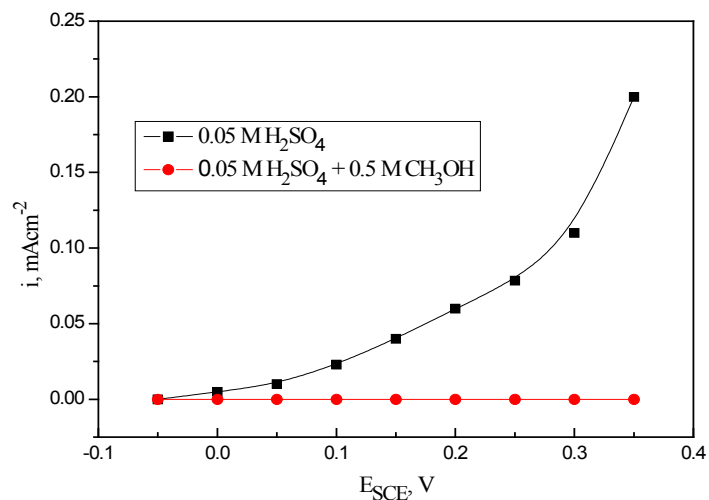


Fig. 10. Potentiodynamic polarization of rhenium oxide electrode in $0.05 \text{ M H}_2\text{SO}_4 + 0.5 \text{ M CH}_3\text{COOH}$ solutions.

Conclusion

- 1- The rate of corrosion of rhenium electrode in the investigated solutions is maximum in NaOH and minimum in Na₂SO₄.
2. The presence of oxygen enhances the dissolution process in the weakly corrosive solution e.g., Na₂SO₄.
3. The pre immersion oxide film grows further in H₃PO₄, and to a larger extent in CH₃COOH. The oxide grown in the high concentration of acetic acid solutions is more compact than that grown in dilute ones.
4. The rate of oxide film growth increases linearly with increasing the acetic acid concentration.
5. Capacitance measurements are a better probe than potential since $\frac{\partial K_C}{\partial C} > \frac{\partial K_E}{\partial C}$, as due to the open structure nature of the oxide.
6. Complex plane analysis of the impedance gives a dielectric loss angle of the oxide in the range 40-58° for the acetic acid concentration range 1-50 mM.
7. The Re oxide grown in the concentrated solutions is more compact or less reactive than that grown in the dilute solutions
8. The activity of the formed Re oxide increase the electro-oxidation of methanol in acidic solution.

Acknowledgments

The authors gratefully acknowledge the approval and support of this research study by the grant no (SCI-2018-3-9-F-7680) from the deanship of science research at Northern Border University, Arar, K.S.A.

References

1. Gorr B., Trindade V. B., Burk S., Christ, H.-J., Oxidation Behavior of Model Cobalt-Rhenium Alloys During Short-Term Exposure to Laboratory Air at Elevated Temperature, *Oxidation of Metals* 7, 157-172(2009).
2. Palmer D.N., Cartwright J.S. and Neil J.K.O²; US 4, 808, 494, Chem. Abst. 111, 10300X (1989).
3. Rivera J.G., Garcia-Garcia R., Coutino-Gonzalez E., Orozco G., *Int. J. Hydrogen Energy*, 44, 27472 (2019).
4. Hämäläinen, K. Mizohata, K. Meinander, M. Mattinen, M. Vehkamäki, J. Räisänen, et al., *Angew Chem. Int. Ed*, 57, 14538 (2018).
5. Yang S.-Z., Gong Y., Manchanda P., Zhang Y.-Y., Ye G., Chen S., et al. *Adv Mater*, 30, 1803477 (2018).
6. Vargas-Uscategui A., Mosquera E., Chornik B., Cifuentes L., *Electrochim. Acta*, 178, 739 (2015).
7. Cazzanelli E., Castriota M., Marino S., Scaramuzza N., Purans J., Kuzmin A., et al, *J. Appl. Phys.* 105, 114904 (2009).
8. Castriota M., Cazzanelli E., Das G., Kalendarev R., Kuzmin A., Marino S., et al., *Mol. Cryst. Liq. Cryst.* 474, 1 (2007).
9. Karan H.I., Sasaki K., Kuttiyiel K., Farberow C., Mavrikakis M., Adzic R.R., *ACS Catal.* 2, 817 (2012).
10. Tayal J., Rawat B., Basu S., *Int. J. Hydrogen Energy* 37, 4597 (2012).
11. Escolastico S., Seeger J., Roitsch S., Ivanova M., Meulenberg W., Serra J.M., *Chem. Sus. Chem.* 6, 1523 (2013).
12. Muñoz E.C., Schrebler R.S., Orellana M.A., Córdova R., *interface, J. Electroanal. Chem.* 611, 35 (2007).
13. Muñoz E.C., Schrebler R.S., Grez P.C., Henríquez R.G., Heyser C.AVerdugo., P.A., et al., *J. Electroanal. Chem.* 633, 113 (2009).
14. Yang X., Koel B.E., Wang H., Chen W., Bartynski R., *ACS Nano* 6, 1404 (2012).
15. Magee K.J. and Cardwell T.J. "in *Encyclopedia of Electrochemistry of the Elements*", (Ed) A.J. Bard, Vol. II, Chap. 4, Marcel Dekker Inc. NY (1976) p. 180.
16. Searcy A.W., Ragone D.V. and Colombo U., Eds., "Chemical and Mechanical Behaviour of Inorganic Materials", Wiley Interscience, New York, (1968).
17. Hefny M.M., *Bull. Electrochem.* 5, 718, (1989).
18. El-Basiouny M.S., El-Kot A. M., Hefny M. M., *Corrosion* 36, 284 (1980).
19. El-Basiouny M.S., and Bekheet A. M., *Br. Corros. J.* 15, 89 (1980).
20. Badawy W.A., Al-Kharafi F.M, *Electrochim. Acta*, 44, 693 (1998).

21. Young L., "Anodic Oxide Films", Academic Press, London, (1961).
22. Greenwood N.N. and Earnshaw A., "Chemistry of the Elements", Pergamon Press, Oxford, p. 1211 (1984).
23. Hefny M.M., El-Basiouny M.S., Gad Allah A.G. and Salih S.A., *Electro chim. Acta*, 28, 1811 (1983).
24. Delahay, P., "Double Layer and Electrode Kinetics", Interscience Publishers, New York, 141 (1966).
25. Moore W.J., "Physical Chemistry", Longman, London, 498 (1978).
26. Hefny M.M., *Appl. Electrochem.* 21, 483, (1991).
27. "Basics of AC Impedance Measurements", Application Note AC-1, EG & G Princeton Applied Research, Electrochemical Instruments Division 1983.
28. Hefny M.M., Abd El Wanees S., *Electrochem. Acta.*, 14, 1419 (1969).

النشاط الحفزي للأقطاب المعدلة في خلايا الوقود . ١. السلوك الكهروكيميائي للرينيوم في ظل ظروف التآكل الطبيعي

محمود جمال ابو بكر صالح^١، صلاح عبد الوونيس^{٢,٣}، سيد خالد مصطفى^٤

^١ قسم الكيمياء. كلية العلوم. جامعة الحدود الشمالية. عرعر - المملكة العربية السعودية

^٢ الكلية الجامعية بأمّالج. أمّالج - جامعة تبوك. تبوك - المملكة العربية السعودية

^٣ قسم الكيمياء. كلية العلوم. - جامعة الزقازيق - مصر

^٤ قسم الكيمياء. كلية العلوم. - جامعة تبوك. تبوك - المملكة العربية السعودية

تم دراسة السلوك الكهروكيميائي لقطب الرينيوم Re في بعض المحاليل المائية باستخدام قياسات الدائرة المفتوحة (السعة C والجهد E) في غياب ووجود الاكسجين ، عند ٢٥ درجة مئوية.

أكدت النتائج ان سطح المعدن مغطى بغشاء أكسيد من المحتمل أن يكون ReO_2 في جميع المحاليل التي تم فحصها باستثناء H_3PO_4 ، و CH_3COOH ، تذوب طبقة أكسيد الرينيوم، بينما ينمو أكسيد الرينيوم في H_3PO_4 ، و CH_3COOH .

تم قياس معدل نمو غشاء الأكسيد في المحاليل مختلفة التركيز من حمض الخليك ووجد أنه يزداد بشكل مباشر مع تركيز الحامض. السمك النسبي لطبقة الأكسيد شكلت حالة مستقرة (بعد حوالي 90 دقيقة من الغمر). اظهرت مقارنة معاملات معدلات تكوين الأكسيد المستمدة من قياسات السعة مع تلك المشتقة من القياسات المحتملة أن بنية الأكسيد يتغير مع تكوين المحلول؛ ربما تتخفف سمك طبقة الأكسيد بزيادة تركيز الحمض. يشير القطب المؤكسد لأكسيد الرينيوم إلى وجود نشاط حفزي جيد تجاه أكسدة الميثانول في المحاليل الحمضية.